

RESEARCH ARTICLE

The horizontal and vertical controls on the thermal structure of the tropical troposphere

L. A. Palmer^{1,2}  | M. S. Singh^{1,2}¹School of Earth, Atmosphere and Environment, Monash University, Melbourne, Victoria Australia²Centre of Excellence for Climate Extremes, Monash University, Melbourne, Victoria Australia**Correspondence**L. A. Palmer, School of Earth, Atmosphere and Environment, Monash University, Melbourne, VIC, Australia.
Email: lucinda.palmer3@gmail.com**Funding information**Australian Research Council,
Grant/Award Numbers: DE190100866,
DP230102077; Climate Extremes,
Grant/Award Number: CE170100023**Abstract**

Our conceptual understanding of the tropical thermal structure is based on two complementary idealisations: one stemming from convective quasi-equilibrium (QE) and the other being the weak temperature gradient (WTG) approximation. Through QE, moist convection provides a vertical control on the thermal structure, while, under WTG, wave dynamics are assumed to provide a non-local horizontal control. While it is clear that moist convection plays an important role in setting the tropical mean stability through QE, the extent to which QE implies a local constraint on stability or whether the requirement for WTG effectively inhibits the influence of local conditions on stability remains debated. Here we hypothesise that a strong local vertical control of the thermal structure would imply a relationship between humidity and stability in the troposphere, as convection within moister regions would be less affected by entrainment of surrounding air. We utilise a combination of ERA5 reanalysis and observational data to examine the relationship between stability and local humidity across the Tropics. The results are compared with a prediction based upon a specific realisation of the theory of QE that incorporates entrainment through a simple plume model. We discover that, in convective regions, wave dynamics do not eliminate the effect of local conditions on stability, and that the resulting relationship between stability and humidity can be approximated well by the entraining plume model. Since QE is not applicable in the absence of convection, in non-convective regions the WTG, and possibly other factors, acts to set stability in the region. These results may help us understand the controls on horizontal density gradients in the tropical troposphere and the associated overturning circulations.

KEYWORDS

convection, entrainment, quasi-equilibrium, tropical stability, weak temperature gradient

1 | INTRODUCTION

In the Tropics there are two key idealisations that ground theoretical understanding of the thermal structure of the troposphere (Bao & Stevens, 2021). The first of these is the assumption that horizontal variations in free-tropospheric

temperature are small. This is known as the weak temperature gradient (WTG) approximation (Sobel *et al.*, 2001): since the influence of rotation in the Tropics is weak, gravity waves are able to remove density anomalies efficiently in the tropical troposphere (Bretherton & Smolarkiewicz, 1989), preventing strong temperature

gradients from being maintained (Charney, 1963). The second idealisation states that, in regions of convection within the Tropics, the thermal structure closely follows that of moist adiabatic ascent (e.g., Emanuel, 2007). This arises as a simplification of the more general concept of convective quasi-equilibrium (QE), the hypothesis that, on sufficiently large scales, moist convective heating remains in rough balance with the large-scale forcing within the Tropics (Arakawa & Schubert, 1974). Together, these idealisations provide a simple picture of the tropical troposphere as having a horizontally homogeneous temperature with a profile close to that of a moist adiabat. It is important, however, to note that both these principles are approximations; research has shown that substantial horizontal gradients in temperature do exist in the tropical troposphere (Bao & Stevens, 2021) and that the thermal structure does not necessarily adhere strictly to a moist adiabat (Mapes, 2001). Therefore, an important challenge in tropical meteorology is to understand the causes and implications of deviations from the moist adiabatic lapse rate and WTG in the observed thermal structure.

The processes that maintain weak temperature gradients within the tropical troposphere include wave dynamics that spread the effect of diabatic heating horizontally (Bretherton & Smolarkiewicz, 1989). Such mechanisms therefore provide a horizontal control on the tropical thermodynamic structure that acts non-locally to reduce density anomalies. However, even under the WTG approximation this does not lead to complete homogenisation of temperature (Figure 1). Firstly, due to the virtual effect of water vapour, when density is horizontally invariant, temperature variations can nevertheless exist due to horizontal variations in moisture (Yang *et al.*, 2022). Moreover, the existence of large-scale overturning circulations implies non-zero density gradients in the free troposphere. For example, Bao and Stevens (2021) showed that temperature variations (and density temperature variations) of 2–4 K are present seasonally in the upper tropical

troposphere over smaller spatial scales than would be expected based on thermal wind balance arguments (e.g., the South Asian High; Wu *et al.*, 2015). These variations may be related hydrostatically to the pressure gradients required to maintain the circulation. Indeed, in studies that apply the WTG approximation to limited-area modelling, temperature anomalies are either implicitly (Kuang, 2008) or explicitly (Raymond & Zeng, 2005) related to large-scale vertical motion. Bao and Stevens (2021) found that the magnitude of the temperature anomalies was smallest in the mid-troposphere, suggesting that the efficacy of gravity waves in homogenising the density is greatest in the mid-troposphere.

To understand deviations from strict WTG, Williams *et al.* (2023) introduced the conceptual “circus tents” model of the free-tropospheric temperature. In this model, temperature in the free troposphere is maintained through moist adiabatic ascent in deep convective regions (the tent poles) and slowly decreases with distance from deep convection (the tent fabric) due to the imperfect efficacy of gravity waves in removing density gradients. This is consistent with previous theoretical models of the response to tropical heating, in which a dissipation term is included to account for the decreasing efficacy of gravity waves with distance from convection (Gill, 1980; Matsuno, 1966). The “circus tents” model therefore suggests that the deviations from temperature homogeneity could be the result of gravity waves failing to eliminate all temperature gradients within the Tropics. Other work has highlighted the importance of balanced dynamics in the Tropics (Adames, 2022; Raymond *et al.*, 2015; Sessions *et al.*, 2019), in which horizontal density gradients may be related to vorticity anomalies in the troposphere through balance conditions such as geostrophic balance or, more appropriately in the Tropics, nonlinear balance (see e.g., Raymond *et al.*, 2015).

In contrast to the above mechanisms, convection has a strong effect on the temperature profile within a given column, providing a local, vertical control on the tropical thermal structure. Here, we think of a “column” of the atmosphere as a region large enough to contain an ensemble of convective clouds rather than a particular location. Through the analysis of soundings from deep convective regions, it was suggested that the action of convection was to bring the vertical temperature profile towards neutrality with respect to a reversible, adiabatic ascent (Betts, 1982; Xu & Emanuel, 1989). Later studies, however, pointed out the sensitivity of this result to the inclusion of ice (Williams & Renno, 1993) and assumptions about microphysics (Bao & Stevens, 2021). Moreover, while undilute ascent within convective cores has previously been seen as an important process for explaining the observed tropical thermodynamic structure

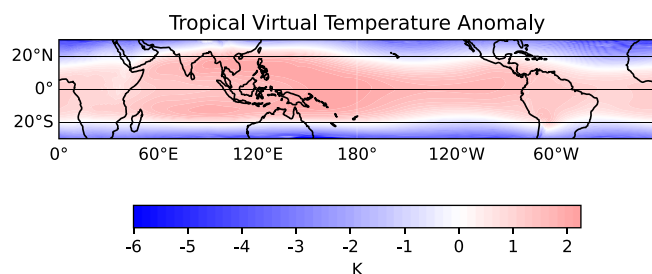


FIGURE 1 The time-mean virtual temperature anomaly at 500 hPa for the years 2000–2019 with respect to the tropical mean temperature at the same level between 30°N and 30°S according to the ERA5 reanalysis. [Colour figure can be viewed at [wileyonlinelibrary.com](https://onlinelibrary.wiley.com)]

(Riehl & Malkus, 1958), observational (Jorgensen & LeMone, 1989; Lucas *et al.*, 1994) and cloud-resolving modelling (Kuang & Bretherton, 2006; Romps & Kuang, 2010) studies have provided evidence that undiluted air parcels are rare in the upper troposphere. Indeed, it has long been known that entrainment and detrainment are key processes that must be considered in the parameterisation of convection (e.g., Arakawa & Schubert, 1974), and considerable effort has been expended on representing entrainment in large-scale models (see the review by de Rooy *et al.*, 2013). This then raises the question of the effect the entrainment of environmental air would have on the tropospheric thermal structure.

To examine the impact of entrainment on the tropical temperature profile, Singh and O’Gorman (2013) introduced the conceptual zero-buoyancy plume (ZBP) model. The model is a simple bulk entraining plume that acts as a highly simplified model of an ensemble of convective clouds, similar to that used in many convective parameterisations (e.g., Tiedtke, 1989). Essentially, the ZBP model assumes that the aggregate effect of convection is to bring the temperature profile to one neutral to an entraining plume rather than a moist adiabat, consistent with the original QE formalism of Arakawa and Schubert (1974). While the model was originally applied to simulations of radiative–convective equilibrium as a model for the mean stratification in the Tropics, if applied locally to given columns it suggests a connection between stability and humidity (Singh *et al.*, 2019). In drier regions, entrainment has a stronger effect on rising air parcels, causing the environment to become more unstable. A number of studies have also reported that tropical lapse rates generally decrease as moisture in the troposphere increases (Gjorgjievska & Raymond, 2014; Raymond *et al.*, 2015; Singh & O’Gorman, 2013), providing some evidence of a relationship between stability and moisture.

The importance of entrainment in moist convection has also been investigated from the inverse perspective, beginning by examining a relationship between convective activity and environmental conditions. It is well known that there is a strong relationship between precipitation and tropospheric moisture in the Tropics (Bretherton *et al.*, 2004; Holloway & Neelin, 2009). By considering the effect of convective entrainment, these relationships were framed in terms of the buoyancy of a hypothetical cloud that mixes with its environment by Ahmed and Neelin (2018). The authors used the observed precipitation–buoyancy relationship to motivate a model for the adjustment of temperature and moisture within the troposphere, finding a relationship between stability and humidity similar to that described by the ZBP model above (Ahmed *et al.*, 2020).

Although there is some evidence for relationships between stability and humidity in the tropical atmosphere that are consistent with the ZBP model, the extent to which this is applicable at given locations in the Tropics remains unclear. Singh *et al.* (2019) showed that the ZBP model performed well in reproducing the results of idealised cloud-resolving model simulations forced by varying degrees of ascent. However, as pointed out by Romps (2021), the simulations did not take into account WTG constraints on the tropical thermal structure and therefore could not be used as a proxy for observed spatial variations; the simulations implied horizontal gradients in temperature across the tropical band much larger than observed. Romps (2021) instead argued that horizontal controls from waves are too strong to allow the effect of entrainment to be observed in spatial variations in the lapse rate; rather, the ZBP model could only be applied to the tropical mean. A later study coupled the entraining plume model with a large-scale circulation to account for the dynamical constraints on the tropical atmosphere (Singh & Neogi, 2022). This study suggested that the ZBP assumption may still be valid locally in the Tropics, even under WTG constraints, thereby raising the possibility that vertical control by tropical convection may partially explain deviations from strict WTG in the troposphere.

In this study, we investigate the horizontal and vertical influences on the thermal structure of the tropical troposphere using both reanalysis and observation data. We show that stability has a non-monotonic dependence on humidity of the troposphere, but, for sufficiently moist regions and in particular for convecting regions, the troposphere becomes more stable with increasing humidity. Within these convective regions, the ZBP model is able to reproduce the relationship for a sufficient entrainment rate, providing evidence that entrainment is an important factor in controlling local lapse rates within convecting regions. Analysis of non-convective regions reveals that local deviations from the WTG exist. Motivated by the “circus tents” model, we explore whether the lapse rates outside convective regions can be understood as being set remotely by nearby convection. However, we find such an explanation to be too simple, and instead we highlight vertical variations in the efficacy of horizontal controls as an important avenue for future work.

The rest of the article is organised as follows. The data used are described in Section 2. In Section 3 we examine the relationship between stability and humidity across the Tropics and in Section 4 we compare these results with the ZBP model. We also study non-convective regions in Section 5 and investigate the local gradients in temperature between convective and non-convective regions. We present a summary and our main conclusions in Section 6.

2 | DATA

The bulk of our analysis utilises the fifth generation of atmospheric reanalyses from the European Centre for Medium-Range Weather Forecasts (ECMWF), ReAnalysis 5 (ERA5: (Hersbach *et al.*, 2020)). Data are provided on a $0.25^\circ \times 0.25^\circ$ grid on 37 pressure levels with hourly time output, which we average to create daily means. We conduct our study over a 20-year period (2000–2019) and focus on the region of the Tropics between 20°N and 20°S . To ensure that we examined regions of sufficient size for the assumption of convective quasi-equilibrium to be valid, we also repeated our analysis by first coarsening the reanalysis to a $1^\circ \times 1^\circ$ grid. However, we find almost identical results in this case, and we therefore only show results on the original reanalysis grid.

We repeat the same analysis using the Modern-Era Retrospective analysis for Research and Application, Version 2 (MERRA2: (Gelaro *et al.*, 2017)). MERRA2 has a $0.5^\circ \times 0.625^\circ$ grid available at 42 pressure levels. Once again, we look at a 20-year period from 2000–2019 and focus on the region of the Tropics between 20°N and 20°S . We average six-hourly data for most variables to construct daily means, except for precipitation, for which we average hourly data to construct daily means.

Finally, we employ radiosonde and station data to examine whether the reanalysis results are supported by observational data. We use the Integrated Global Radiosonde Archive (IGRA: (Durre *et al.*, 2016)) for our free-tropospheric variables and combine this with observed station precipitation data from the Global Historical Climate Network (GHCN: (Menne *et al.*, 2012)). We analyse 71 stations between 20°N and 20°S that are featured in both IGRA and GHCN. When studying the data from the IGRA, we take only soundings that provide temperature, humidity, and height at 1000, 850, 700, and 500 hPa and discard soundings that do not contain all these data. We consider days for which there are at least two sounding launches, and we average all daily soundings together to construct an approximate daily mean. The GHCN contains daily data, so no averaging for the dataset was completed.

3 | EVIDENCE FOR A VERTICAL CONTROL ON THE THERMAL STRUCTURE IN CONVECTING REGIONS

We first examine relationships between stability and humidity in the tropical troposphere by compositing thermodynamic and dynamic profiles from ERA5 based on the lower-tropospheric moisture. We construct profiles

of relative humidity, virtual temperature (using density temperature produces almost identical results), and pressure vertical velocity anomalies as a function of the lower-tropospheric relative humidity (Figure 2). Here the lower tropospheric relative humidity is taken as the weighted average of the humidity at pressure levels between 850 and 500 hPa.

The relative humidity throughout the column increases with the lower-tropospheric relative humidity (Figure 2a), consistent with previous work demonstrating that variability in column humidity is driven by variations in the lower troposphere (Holloway & Neelin, 2009). In addition, the pressure velocity becomes increasingly negative, implying stronger upward motion, throughout the troposphere as the lower-tropospheric humidity increases (Figure 2b), particularly for the highest relative humidity bin (90%–100%). To the extent that large-scale upward motion is indicative of strong precipitation and convection (Louf *et al.*, 2019), this is also consistent with much previous work on the relationship between humidity and precipitation in tropical regions (Bretherton *et al.*, 2004; Holloway & Neelin, 2009; Rushley *et al.*, 2018).

Interesting relationships are found between the lower-tropospheric relative humidity and the virtual temperature. The virtual temperature anomaly profiles vary strongly with humidity (Figure 2c). However, in the lower troposphere the variation is not monotonic. At low relative humidity, the virtual temperature anomaly is strongly negative at low levels, while for lower-tropospheric relative humidity values between 70% and 80% the anomalies are positive. At even higher lower-tropospheric relative humidity, the virtual temperature anomaly near the surface again becomes negative. At higher levels, different behaviour is seen; near 600 hPa, little variation in virtual temperature with humidity is seen, while above this level the virtual temperature anomaly increases monotonically with humidity. Since the static stability within the troposphere is directly related to the change in virtual temperature with height, these results imply changes in the stability of the troposphere as a function of the relative humidity. Comparing virtual temperature anomalies in the lower and upper troposphere, the results suggest that the most unstable profiles occur under moderate relative humidity, with both the moistest and driest columns being more stable. In particular, for columns with humidities above 70%, corresponding to large-scale upward motion (Figure 2b), the atmosphere becomes more stable as humidity increases.

The profiles seen above may be compared with the theoretical profiles described in Singh and Neogi (2022). They developed a model for the thermodynamic and dynamic structure of the ascending branch of a large-scale

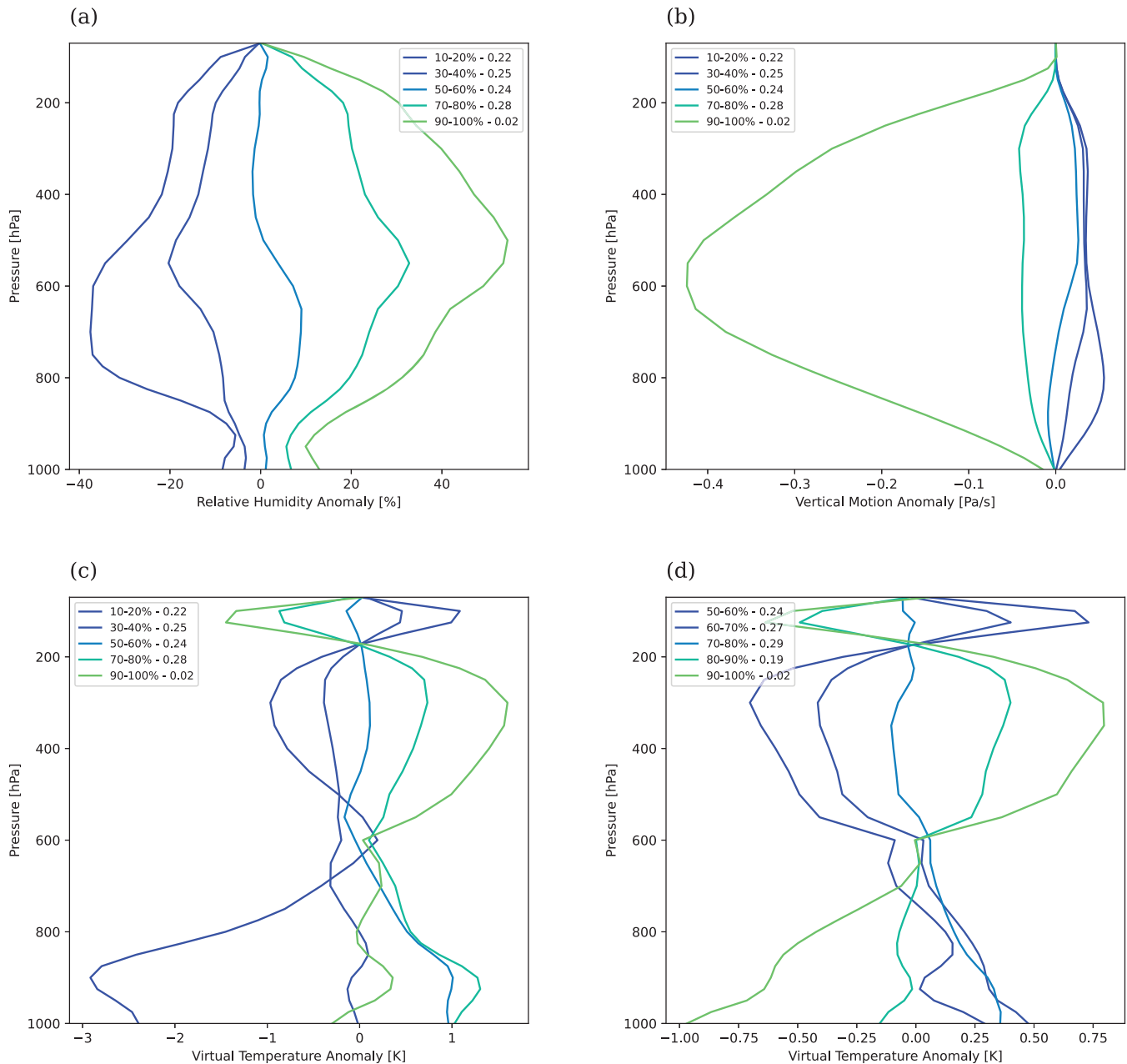


FIGURE 2 (a) Relative humidity anomalies, (b) pressure velocity, and (c,d) virtual temperature anomalies binned by lower-tropospheric relative humidity according to ERA5 as given in the legend. Lower-tropospheric relative humidity is taken as the pressure-weighted mean relative humidity between 850 and 500 hPa. Anomalies in (a)–(c) are taken with respect to the tropical and time mean and those in (d) are taken with respect to the tropical and time mean for regions with lower-tropospheric relative humidity greater than 50%. Numbers following relative humidity ranges in the legend give the fraction of points in each bin. [Colour figure can be viewed at wileyonlinelibrary.com]

circulation using the ZBP model coupled to a dynamic model based on the WTG approximation. In particular, they showed that the ascending branch has a higher tropospheric relative humidity than the tropical mean, alongside temperature anomalies that are negative at low levels and positive at high levels, implying a more stable troposphere than the tropical mean. Indeed a similar profile of virtual temperature anomalies is produced in the ascent

region when we consider only regions of the atmosphere in which the lower-tropospheric relative humidity is greater than 50% (Figure 2d); the most moist regions have negative anomalies near the surface and positive anomalies of virtual temperature above 600 hPa. The virtual temperature profiles found in ERA5 are therefore qualitatively consistent with the behaviour of the ZBP model, in which entrainment plays a key role in setting the lapse rate,

motivating us to apply this model to help explain the reanalysis data in the next section.

4 | COMPARISON WITH THE ZERO-BUOYANCY PLUME MODEL

The ZBP model assumes that the environment of convection adjusts to a state neutral to an entraining plume. This implies that the saturation moist static energy (MSE^*) of the troposphere above cloud base obeys the plume equation,

$$\frac{dMSE^*}{dz} = -\epsilon L_v(q^* - q), \quad (1)$$

where ϵ is the entrainment rate, $MSE^* = c_p T + gz + L_v q^*$ is the saturation moist static energy, $q^* - q$ is the saturation deficit, and z is the height. Here c_p is the isobaric specific heat capacity of air, L_v is the latent heat of vaporisation, T is the temperature, q is the specific humidity, q^* is the saturation specific humidity, and g is the gravitational acceleration. Equation (1) neglects virtual effects, which can be important in evaluating horizontal gradients in buoyancy (Yang *et al.*, 2022). However, here we are interested in vertical gradients in temperature and density, for which the virtual effect is small; the neglect of virtual effects has been used successfully in a number of previous studies with the ZBP model (Romps, 2014, 2016; Singh & Neogi, 2022).

Integrating in the vertical between two levels, where entrainment and the latent heat of vaporisation are taken to be constant with height, we may write

$$\Delta MSE^* = -\epsilon \Delta z \overline{L_v(q^* - q)}, \quad (2)$$

where ΔMSE^* is the change in MSE between the two levels separated by a height difference Δz , and the overbar represents a height-weighted mean.

The above equation implies that the vertical change in MSE^* is directly related to the saturation deficit. MSE^* is a function of temperature, pressure, and height only, and so its variation in the vertical is a measure of stability. If MSE^* is invariant with height, the stability is moist adiabatic, whereas if it decreases with height the atmosphere is more unstable than a moist adiabat. The saturation deficit, on the other hand, is a measure of humidity, with zero saturation deficit implying saturated conditions. In this way, the ZBP model implies a relationship between stability and humidity. We focus here on the mid to lower troposphere, and we consider the interval between 850 and 500 hPa.

Figure 3 shows solutions of Equation (2) for three different entrainment rates of 0.1, 0.25, and 0.5 km^{-1} , chosen to span the ΔMSE^* and saturation deficit values we find in

ERA5 below and calculated based on a height difference of approximately 4 km, given by the average height difference between 850 and 500 hPa in the tropical band (20°S–20°N) in ERA5. The model predicts a linear relationship between the stability (as measured by ΔMSE^*) and the humidity (as measured by the saturation deficit). For zero saturation deficit, entrainment has no effect on the ZBP and ΔMSE^* is zero.

We can now compare the ZBP solutions with data from ERA5 and the IGRA. We calculate MSE^* from daily-averaged profiles of temperature and geopotential height over the interval 850–500 hPa. We evaluate the saturation deficit over the same region using a height-weighted average, and we multiply by the latent heat of vaporisation to convert to energy units.

We construct a 2D histogram, plotting the values of the change in MSE^* against the corresponding saturation deficit and overlaying the ZBP solutions onto the ERA5 distribution. Immediately, there is a clear correlation between the change in MSE^* and the saturation deficit, where more instability occurs in regions and at times where the troposphere is drier (Figure 3a). Although there is considerable scatter in the points, for small values of the saturation deficit and change in MSE^* there appears to be a relatively linear relationship between ΔMSE^* and saturation deficit, bounded by the ZBP solutions for entrainment rates of 0.10 and 0.50 km^{-1} .

To determine whether a similar relationship is found in direct observations, we construct the same histogram based on the IGRA radiosonde data. There is considerably more scatter in the points, and any relationship is less clear. This is partly simply because of the lack of data; only 71 stations are available between 20°N and 20°S, and this gives a total number of 240,515 profiles compared with 1.68 billion in ERA5. Additionally, since the radiosondes give point measurements rather than averages, the humidity they measure may not be representative of the average environment for convection and may be moister or drier. This could lead to more scatter in the histogram, even if the fundamental relationship is present in the observed data.

Despite the above caveats, the region of highest frequencies of occurrence tends to be approximately elongated along the ZBP solution of 0.25 km^{-1} . Though not conclusive, the results suggest that the humidity–stability relationship found in ERA5 is not simply an artifact of the reanalysis. Note that the saturation deficit values for the radiosonde data appear to be generally higher than those for the reanalysis. This is due to differences between the distributions of saturation deficit in the observations and the reanalysis, with the radiosondes leaning towards larger saturation deficits. It is possible that an actual difference in these values exists between the soundings and reanalysis, although it may also be due to the single point values in

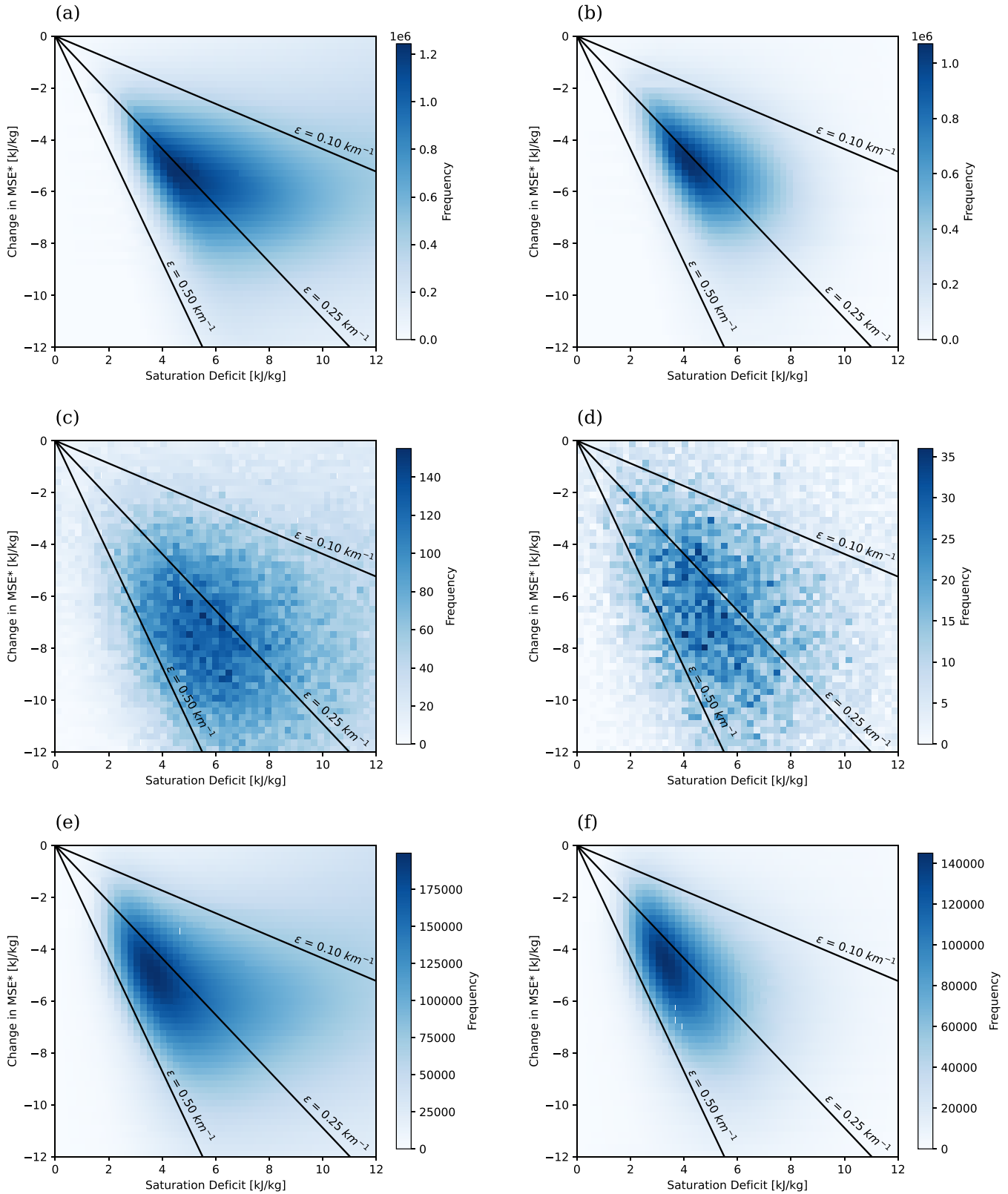


FIGURE 3 2D histograms depicting the relationship between the change in MSE^* and the saturation deficit between 850 and 500 hPa. Solid lines give solutions of the ZBP model for varying entrainment rates as labelled. We show the results from (a,b) ERA5, (c,d) IGRA radiosonde data, and (e,f) MERRA2. (a,c,e) include all points with the domain (20°N – 20°S) and (b,d,f) include only points exceeding the precipitation threshold of $5\text{ mm}\cdot\text{day}^{-1}$. [Colour figure can be viewed at wileyonlinelibrary.com]

the soundings differing from the area average in the ERA5 reanalysis.

Note that Singh and O’Gorman (2013) also examined the extent to which the stability of atmospheric soundings could be understood using the ZBP, using radiosonde measurements from the tropical western Pacific. They found that an entrainment profile of $\epsilon = 1.5/z$ roughly corresponded to the most unstable lapse rates in the lower troposphere. Here we focus on the bulk of the distribution, and as a result we find lower values of the entrainment rate.

Finally, we also computed the stability–humidity histogram in a second reanalysis (MERRA2). Although the entrainment values that encompassed the data appear slightly different from those for ERA5, the overall relationship remains clear (Figure 3e, f).

At higher values of the saturation deficit, the spread in the data becomes larger, and the relationship between ΔMSE^* and the saturation deficit deviates from that predicted by the ZBP model. One possible reason for this is that the ZBP model is only properly representative of convective regions. Since the ZBP model assumes that the atmosphere is rapidly brought to neutrality with respect to convection, it is only valid where convection is active. We therefore examine how the histogram is altered if we only consider regions where moist convection is present. We use total precipitation in ERA5 (convective and large-scale) as a proxy for convection and set a threshold of $5 \text{ mm}\cdot\text{day}^{-1}$ to exclude regions where moist convection is not occurring. With this idea now in mind, we plot the ERA5 distribution including only regions that exceed the precipitation threshold (Figure 3b). With precipitation generally occurring in more moist atmospheres, this removes much of the scatter of the distribution observed at values of greater saturation deficit. The resulting figure now has a stronger linear relationship between the change in MSE^* and the saturation deficit. The distribution is centred around the ZBP solution of 0.25 km^{-1} , but a range of values for entrainment exist. These results suggest that selecting a single value for entrainment in convective parameterisations may not cover all tropical variance; however, it may still be able to capture the mean distribution.

When we consider only precipitating regions in the radiosonde data, as given by a daily precipitation rate larger than 5 mm according to the GHCN database, the histogram appears slightly more aligned with the ZBP solutions, but remains relatively unchanged. The reasons for this are possibly to do with the lack of data and representation errors discussed earlier. The sensitivity of the distribution to the precipitation threshold for both the reanalysis datasets and observations was also tested. Upon increasing the threshold, the spread of the distribution along its slope

decreases; however, the slope of the distribution ultimately remains the same.

Based on the above results, we suggest that the ZBP model provides an explanation for some of the variation in lapse rates in regions of precipitation. Outside these regions, one does not expect convection to control the lapse rate, and the ZBP performs poorly as a result. In non-precipitating regions, it is likely that horizontal controls on the thermal structure can effectively inhibit differences in stability between regions of varying humidity. We now investigate these horizontal controls in more detail.

5 | HORIZONTAL CONTROLS ON THE THERMAL STRUCTURE IN NON-CONVECTIVE REGIONS

The conceptual “circus tents” model introduced by Williams *et al.* (2023) suggests that MSE^* in the free troposphere is communicated horizontally via gravity waves from convective to non-convective regions. This establishes a threshold for convection for regions in the vicinity of active convection, so that convection cannot occur unless the MSE in the sub-cloud layer is equal to or greater than the communicated value of free-tropospheric MSE^* . Whilst according to this model the threshold for convection decreases with distance from the active convection, we can expect that non-convective regions nearby would have roughly similar MSE^* to the convective area. To test the extent of this horizontal control, we examine correlations between the tropospheric MSE^* in convecting regions with their surrounds, as a function of distance. We expect the correlation to decrease with distance, but, given typical speeds of gravity waves that span the troposphere ($\sim 50 \text{ m}\cdot\text{s}^{-1}$: Fulton and Schubert (1985); Mapes and Houze (1995)), we expect homogenisation of temperature to some degree at distances exceeding 2000 km at daily time-scales.

We choose grid points with less than $5 \text{ mm}\cdot\text{day}^{-1}$ of total precipitation to be our non-precipitating points. From each non-precipitating grid point we define a “doughnut”-shaped band 60 km wide centred on a given distance. We then calculate the Pearson correlation coefficient between the value of MSE^* at 500 hPa at non-precipitating points and the average MSE^* in subsets of points in the corresponding doughnut. We consider five distances ranging from $120\text{--}2000 \text{ km}$, while limiting the analysis to latitudes between 20°N and 20°S , and we consider three different subsets: non-convective points, the 10% weakest precipitating grids (that still exceed the precipitation threshold), and the 10% strongest precipitating grids. Following the “circus tents” model, we expect the strongly precipitating points to have the most influence on

the non-convective point and therefore have the strongest correlation value.

The resulting correlations depicted in Figure 4 are intriguing. The correlation does decrease with distance as is hypothesised in the “circus tents” model; however, the highest correlation values occur between non-convective points and other non-convective points. In fact, the weakest correlation values occur for the strongly precipitating group, which is in opposition to the “circus tents” model. The reasons for this are unclear, although it may simply be due to the fact that the thermal structure for non-convective points is more similar to that for other non-convective points than for strongly convecting points. Ultimately, the fact that non-convective points are less correlated with convective points at all distances suggests that the gravity-wave adjustment process envisaged by the “circus tents” model is not simple, and one must consider its detailed dynamics explicitly.

After observing the correlations at 500 hPa, we were intrigued by the size of local temperature gradients between non-convective and nearby convective points and how this compares for the rest of the free troposphere. As pointed out by Bao and Stevens (2021), the efficacy of gravity waves to reduce temperature gradients differs throughout the troposphere, so temperature gradients may be more pronounced at certain heights. Gravity waves may therefore be more efficient at reducing temperature gradients in the mid-troposphere compared with the lower troposphere and the boundary layer. To test this theory,

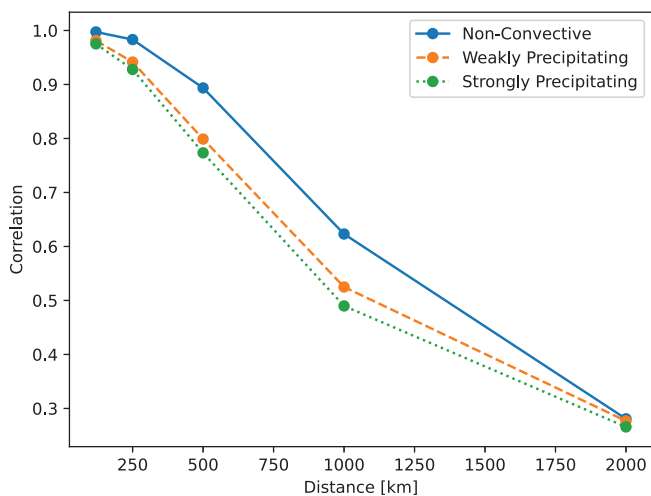


FIGURE 4 Correlation between values of MSE^* at 500 hPa in non-convective regions and the average MSE^* for surrounding non-convective points (solid line), the 10% most weakly precipitating points (dashed line), and the 10% most strongly precipitating points (dotted line) as a function of distance. The average surrounding MSE^* is evaluated in a doughnut 60 km wide centred on the given distance. [Colour figure can be viewed at [wileyonlinelibrary.com](https://onlinelibrary.wiley.com/terms-and-conditions)]

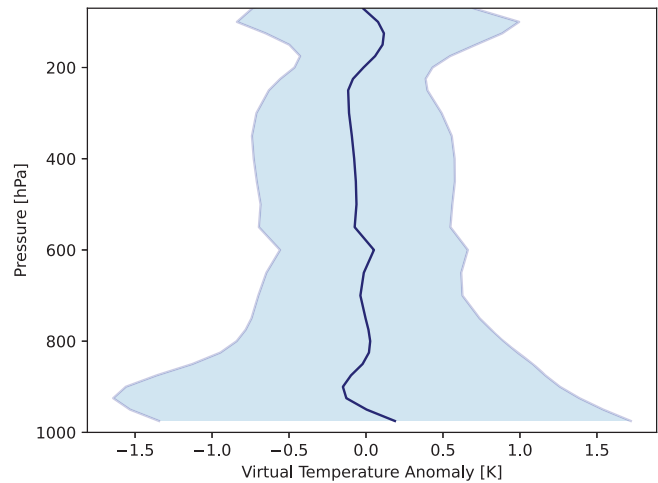


FIGURE 5 The average vertical profile (middle solid line) of the difference in virtual temperature between non-precipitating regions and precipitating regions within 500 km of each non-precipitating point. Shading shows one standard deviation from the mean. [Colour figure can be viewed at [wileyonlinelibrary.com](https://onlinelibrary.wiley.com/terms-and-conditions)]

we examine the spread in temperature differences between non-precipitating points and precipitating points that are within 500 km. At this distance the correlation values are still high and we also expect gravity waves to have travelled this distance on daily time-scales. To focus on differences in density, we consider the profile of differences in virtual temperature between non-precipitating grid points and precipitating grid points within 500 km (Figure 5).

In the mean, temperature gradients are mostly removed locally between precipitating and non-precipitating regions at all levels in the troposphere. However, when we examine the standard deviation of the temperature differences, there is more variation in the boundary layer and the bottom of the lower troposphere than there is in the rest of the troposphere. As well as this, the standard deviation also implies that locally temperature gradients persist between precipitating and non-precipitating points at a 500-km scale, with differences ranging from ± 1.5 K in the lower troposphere to ± 0.5 K in the upper troposphere. This analysis was also repeated for the 90th and 99th percentiles of precipitation instead of all precipitating points, however, this did not have any impact on the spread of the temperature gradients or the mean temperature gradient. In addition to this, given that temperature anomalies appear to depend on the humidity of the environment in some complex way, as seen in Figure 2c, the relationship between the difference in virtual temperature and the precipitation rate between convective and non-convective points was examined. However, temperature differences were found to have roughly the same mean and variance regardless of the precipitation rate of the convective point.

These results demonstrate that, at least on daily time-scales, strongly precipitating points do not influence the free-tropospheric temperature in the simple way one would expect from the “circus tents” model. As well as this, a strict WTG cannot be used to approximate the thermal structure of non-precipitating points precisely, although it is a reasonable first estimate. As depicted in Figure 5, deviations from strict WTG exist at local scales and the magnitude of these deviations varies with height. Therefore, it can be concluded that understanding the deviations from the WTG, as well as how these depend on height, is important for understanding the thermal structure of regions outside moist convection.

6 | CONCLUSION

In this study we have investigated how both horizontal and vertical controls on the thermal structure of the tropical troposphere affect stability and its variations. Vertical profiles of virtual temperature for varying mid-tropospheric humidities demonstrated a variation in thermal stratification with environmental moisture. This was shown to be non-monotonic in the lower troposphere, but monotonic above 600 hPa. Investigating the influence of moist convection on stability further, we identified a relationship between stability and humidity in precipitating regions, with greater instability present in drier atmospheres. The idealised ZBP model was able to reproduce the slope of the relationship between the two variables with an entrainment rate of 0.25 km^{-1} . Outside convecting regions, the ZBP model cannot be applied to describe the thermal structure, as it was formulated under the assumption of QE. Instead the thermal structure in non-convecting regions was theorised to be influenced by the reduction of temperature gradients via gravity waves. Whilst, on average, temperature differences between non-convecting and nearby convecting regions are small, there was considerable variability in these temperature gradients. This variability was greater in the lower troposphere compared with the mid-troposphere.

Our results support findings that entrainment impacts the thermal structure, and thereby also support the idea that ascent within convective clouds is far from being moist adiabatic. In addition, our results provide support for the local applicability of the ZBP model to regions of convection within the Tropics. Whilst this model captures the potential cause for the deviations from strict moist neutrality in convecting regions, the mechanisms controlling horizontal temperature gradients in non-convecting regions are less obvious. We have shown that, on average, the virtual temperature is close to equal

between convecting regions and those nearby, but there is considerable variability around this mean. Our results suggest that the rate at which the communicated value of MSE^* decreases away from convective regions may vary with height in the troposphere. Furthermore, temperatures in non-convective regions are least correlated with the strongest nearby convection, implying that a simple model, such as the “circus tents” model, may not be able to describe the influences on the thermal structure accurately in the absence of convection.

Whilst we have observed deviations from a strict WTG, possibly caused by the efficacy of gravity waves (Bao & Stevens, 2021), this does not explain what sets the local thermal structure in non-convective regions. Another possible approach is to consider the balanced component of the flow, which may be directly related to density gradients through hydrostatic balance, highlighting the influence of vorticity anomalies on the temperature field (Raymond *et al.*, 2015).

While we have focused on entrainment as a key explanation for the relationships between stability and humidity seen in our study, alternative mechanisms that may contribute to this relationship should be mentioned. In particular, variations in convective organisation with humidity may play an important role in setting variations in stability across convective regions. This may occur through variations in entrainment induced by organisation (Becker *et al.*, 2018), but may also occur due to different vertical profiles of convective heating associated with organised convection compared with disorganised convection (e.g., Houze Jr (1989)). Further, studies have shown that the efficacy of convection at adjusting the tropospheric temperature is not perfect, and in fact is weaker in the upper troposphere than the lower troposphere (e.g., Raymond & Herman, 2011; Tulich & Mapes, 2010). This implies that other processes, such as cloud–radiative heating, may also affect the stratification and affect it differently in different regions. However, such variations in radiative or convective heating are likely to be most important in the upper troposphere, while here we have focused mainly on the lower to mid-troposphere.

Despite our lower-tropospheric focus, our results may nevertheless be relevant for the temperature structure of the upper troposphere. For example, climate models are known to overestimate upper-tropospheric temperature trends relative to radiosondes and satellite observations (Keil *et al.*, 2021; Miyawaki *et al.*, 2020). One possible mechanism that would lead to this overestimation is an incorrect representation of entrainment in moist convection (Miyawaki *et al.*, 2020). Our results therefore provide a possible observational constraint on convective entrainment that could be used to test this hypothesis. The entrainment values of 0.1 and 0.5 km^{-1} that bound

the stability–humidity relationship for ERA5 are broadly in line with previous estimates of entrainment in the literature. While large-eddy simulation studies typically find higher values when entrainment is measured directly based on mass exchange between clouds and their environment (Dawe & Austin, 2011; Romps, 2010; Wang, 2020), estimates using the bulk-plume equations are often in the range 0.1–0.5 km⁻¹ in the lower troposphere for deep convection (de Rooy *et al.*, 2013; Romps, 2010). Luo *et al.* (2010) used satellite observations to estimate entrainment rates, finding values < 0.1 km⁻¹ for the deepest convection and in the range 0.1–0.5 km⁻¹ for congestus clouds. However, the extent to which these estimates can be compared directly with the implied entrainment rates found here is unclear. Instead, our results could be used more directly as a constraint on large-scale models, in a similar way to that proposed by Ahmed and Neelin (2018). A possible pathway for future work is therefore to examine the stability–saturation deficit phase space within climate models and explore the implications for models that are unable to reproduce the reanalysis results found here.

Finally, an important open question is to understand the causes of horizontal temperature gradients in the tropical atmosphere in regions far from convection. Previous work has related such gradients to the momentum budget (Bao *et al.*, 2022), balanced dynamics (Adames, 2022), and the linear response to convective heating (Keil *et al.*, 2023), but a simple model such as the “circus tents” model that can provide quantitative predictions of gradients remains elusive.

ACKNOWLEDGEMENTS

We acknowledge the European Centre for Medium-Range Weather Forecasts, which is responsible for ERA5, as well as the National Aeronautics and Space Administration, which is responsible for MERRA2. We also acknowledge the National Centers for Environmental Information, which is responsible for IGRA and GHCN. In addition, we thank Larissa Back and two anonymous reviewers for their insightful comments. We acknowledge support from the Australian Research Council and the Centre of Excellence for Climate Extremes through grant nos. CE170100023 and DP230102077, as well as computational resources and services from the National Computational Infrastructure, all funded by the Australian Government.

CONFLICTS OF INTEREST

The authors declare no conflict of interest.

DATA AVAILABILITY STATEMENT

The European Centre for Medium-Range Weather Forecasts ERA5 reanalysis dataset used in this study is available

at <https://cds.climate.copernicus.eu/cdsapp#!/dataset/reanalysis-era5-complete?tab=form>. The Modern-Era Retrospective analysis for Research and Application, Version 2 (MERRA2) reanalysis dataset used is available at <https://disc.gsfc.nasa.gov/datasets?project=MERRA-2>. The Integrated Global Radiosonde Archive (IGRA) dataset used is available at <https://www.ncei.noaa.gov/data/integrated-global-radiosonde-archive/access/data-por/> and the Global Historical Climate Network (GHCN) dataset used is available at <https://www.ncei.noaa.gov/data/global-historical-climatology-network-daily/access/>. Scripts and programming used for the analysis in the current study are available from the Monash Bridges repository at <https://doi.org/10.26180/27129822.v2>.

ORCID

L. A. Palmer  <https://orcid.org/0009-0004-0403-2031>

REFERENCES

- Adames, Á.F. (2022) The basic equations under weak temperature gradient balance: formulation, scaling, and types of convectively coupled motions. *Journal of the Atmospheric Sciences*, 79, 2087–2108.
- Ahmed, F., Adames, Á.F. & Neelin, J.D. (2020) Deep convective adjustment of temperature and moisture. *Journal of the Atmospheric Sciences*, 77, 2163–2186.
- Ahmed, F. & Neelin, J.D. (2018) Reverse engineering the tropical precipitation–buoyancy relationship. *Journal of the Atmospheric Sciences*, 75, 1587–1608.
- Arakawa, A. & Schubert, W.H. (1974) Interaction of a cumulus cloud ensemble with the large-scale environment, part I. *Journal of the Atmospheric Sciences*, 31, 674–701.
- Bao, J., Dixit, V. & Sherwood, S.C. (2022) Zonal temperature gradients in the tropical free troposphere. *Journal of Climate*, 35, 7937–7948.
- Bao, J. & Stevens, B. (2021) The elements of the thermodynamic structure of the tropical atmosphere. *Journal of the Meteorological Society of Japan. Ser. II*, 99, 1483–1499.
- Becker, T., Bretherton, C.S., Hohenegger, C. & Stevens, B. (2018) Estimating bulk entrainment with unaggregated and aggregated convection. *Geophysical Research Letters*, 45, 455–462.
- Betts, A.K. (1982) Saturation point analysis of moist convective overturning. *Journal of the Atmospheric Sciences*, 39, 1484–1505.
- Bretherton, C.S., McCaa, J.R. & Grenier, H. (2004) A new parameterization for shallow cumulus convection and its application to marine subtropical cloud-topped boundary layers. Part I: description and 1D results. *Monthly Weather Review*, 132, 864–882.
- Bretherton, C.S. & Smolarkiewicz, P.K. (1989) Gravity waves, compensating subsidence and detrainment around cumulus clouds. *Journal of the Atmospheric Sciences*, 46, 740–759.
- Charney, J.G. (1963) A note on large-scale motions in the tropics. *Journal of the Atmospheric Sciences*, 20, 607–609.
- Dawe, J.T. & Austin, P.H. (2011) Interpolation of les cloud surfaces for use in direct calculations of entrainment and detrainment. *Monthly Weather Review*, 139, 444–456.
- de Rooy, W.C., Bechtold, P., Fröhlich, K., Hohenegger, C., Jonker, H., Mironov, D. *et al.* (2013) Entrainment and detrainment in

- cumulus convection: an overview. *Quarterly Journal of the Royal Meteorological Society*, 139, 1–19.
- Durre, I., Yin, X., Vose, R.S., Applequist, S., Arnfield, J., Korzeniewski, B. et al. (2016) Integrated Global Radiosonde Archive (IGRA). Version 2.
- Emanuel, K. (2007) Quasi-equilibrium dynamics of the tropical atmosphere. In: Schneider, T. & Sobel, A.H. (Eds.) *The Global Circulation of the Atmosphere*, Vol. 7. Princeton, NJ: Princeton University Press, pp. 186–218.
- Fulton, S.R. & Schubert, W.H. (1985) Vertical Normal mode transforms: theory and application. *Monthly Weather Review*, 113, 647–658.
- Gelaro, R., McCarty, W., Suárez, M.J., Todling, R., Molod, A., Takacs, L. et al. (2017) The modern-era retrospective analysis for research and applications, version 2 (MERRA-2). *Journal of Climate*, 30, 5419–5454.
- Gill, A.E. (1980) Some simple solutions for heat-induced tropical circulation. *Quarterly Journal of the Royal Meteorological Society*, 106, 447–462.
- Gjorgjievska, S. & Raymond, D.J. (2014) Interaction between dynamics and thermodynamics during tropical cyclogenesis. *Atmospheric Chemistry and Physics*, 14, 3065–3082.
- Hersbach, H., Bell, B., Berrisford, P., Hirahara, S., Horányi, A., Muñoz-Sabater, J. et al. (2020) The ERA5 global reanalysis. *Quarterly Journal of the Royal Meteorological Society*, 146, 1999–2049.
- Holloway, C.E. & Neelin, J.D. (2009) Moisture vertical structure, column water vapor, and tropical deep convection. *Journal of the Atmospheric Sciences*, 66, 1665–1683.
- Houze, R.A., Jr. (1989) Observed structure of mesoscale convective systems and implications for large-scale heating. *Quarterly Journal of the Royal Meteorological Society*, 115, 425–461.
- Jorgensen, D.P. & LeMone, M.A. (1989) Vertically velocity characteristics of oceanic convection. *Journal of the Atmospheric Sciences*, 46, 621–640.
- Keil, P., Schmidt, H., Stevens, B. & Bao, J. (2021) Variations of tropical lapse rates in climate models and their implications for upper tropospheric warming. *Journal of Climate*, 34, 9747–9761.
- Keil, P., Schmidt, H., Stevens, B., Byrne, M.P., Segura, H. & Putrasahan, D. (2023) Tropical tropospheric warming pattern explained by shifts in convective heating in the matsuno–gill model. *Quarterly Journal of the Royal Meteorological Society*, 149, 2678–2695.
- Kuang, Z. (2008) Modeling the interaction between cumulus convection and linear gravity waves using a limited-domain cloud system-resolving model. *Journal of the Atmospheric Sciences*, 65, 576–591.
- Kuang, Z. & Bretherton, C.S. (2006) A mass-flux scheme view of a high-resolution simulation of a transition from shallow to deep cumulus convection. *Journal of the Atmospheric Sciences*, 63, 1895–1909.
- Louf, V., Jakob, C., Protat, A., Bergemann, M. & Narsey, S. (2019) The relationship of cloud number and size with their large-scale environment in deep tropical convection. *Geophysical Research Letters*, 46, 9203–9212.
- Lucas, C., Zipser, E.J. & LeMone, M.A. (1994) Convective available potential energy in the environment of oceanic and continental clouds: correction and comments. *Journal of the Atmospheric Sciences*, 51, 3829–3830.
- Luo, Z.J., Liu, G.Y. & Stephens, G.L. (2010) Use of A-train data to estimate convective buoyancy and entrainment rate. *Geophysical Research Letters*, 37, L09804.
- Mapes, B.E. (2001) Water's two height scales: the moist adiabat and the radiative troposphere. *Quarterly Journal of the Royal Meteorological Society*, 127, 2353–2366.
- Mapes, B.E. & Houze, R.A. (1995) Diabatic divergence profiles in Western Pacific mesoscale convective systems. *Journal of the Atmospheric Sciences*, 52, 1807–1828.
- Matsuno, T. (1966) Quasi-geostrophic motions in the equatorial area. *Journal of the Meteorological Society of Japan. Ser. II*, 44, 25–43.
- Menne, M.J., Durre, I., Korzeniewski, B., McNeill, S., Thomas, K., Yin, X. et al. (2012) *Global Historical Climatology Network - Daily (GHCN-Daily)*, Version 3. Asheville, NC: National Centers for Environmental Information.
- Miyawaki, O., Tan, Z., Shaw, T.A. & Jansen, M.F. (2020) Quantifying key mechanisms that contribute to the deviation of the tropical warming profile from a moist Adiabat. *Geophysical Research Letters*, 47, e2020GL089136.
- Raymond, D., Fuchs, Ž., Gjorgjievska, S. & Sessions, S. (2015) Balanced dynamics and convection in the tropical troposphere. *Journal of Advances in Modeling Earth Systems*, 7, 1093–1116.
- Raymond, D.J. & Herman, M.J. (2011) Convective quasi-equilibrium reconsidered. *Journal of Advances in Modeling Earth Systems*, 3, M08003.
- Raymond, D.J. & Zeng, X. (2005) Modelling tropical atmospheric convection in the context of the weak temperature gradient approximation. *Quarterly Journal of the Royal Meteorological Society*, 131, 1301–1320.
- Riehl, H. & Malkus, J.S. (1958) On the heat balance in the equatorial trough zone. *Geophysica*, 6, 503–538.
- Romps, D.M. (2010) A direct measure of entrainment. *Journal of the Atmospheric Sciences*, 67, 1908–1927.
- Romps, D.M. (2014) An analytical model for tropical relative humidity. *Journal of Climate*, 27, 7432–7449.
- Romps, D.M. (2016) Clausius-Clapeyron scaling of CAPE from analytical solutions to RCE. *Journal of the Atmospheric Sciences*, 73, 3719–3737.
- Romps, D.M. (2021) Ascending columns, WTG, and convective aggregation. *Journal of the Atmospheric Sciences*, 78, 497–508.
- Romps, D.M. & Kuang, Z. (2010) Nature versus nurture in shallow convection. *Journal of the Atmospheric Sciences*, 67, 1655–1666.
- Rushley, S.S., Kim, D., Bretherton, C.S. & Ahn, M. (2018) Reexamining the nonlinear moisture-precipitation relationship over the tropical oceans. *Geophysical Research Letters*, 45, 1133–1140.
- Sessions, S.L., Sentić, S. & Raymond, D.J. (2019) Balanced dynamics and moisture quasi-equilibrium in DYNAMO convection. *Journal of the Atmospheric Sciences*, 76, 2781–2799.
- Singh, M.S. & Neogi, S. (2022) On the interaction between moist convection and large-scale ascent in the tropics. *Journal of Climate*, 35, 4417–4435.
- Singh, M.S. & O’Gorman, P.A. (2013) Influence of entrainment on the thermal stratification in simulations of radiative-convective equilibrium. *Geophysical Research Letters*, 40, 4398–4403.
- Singh, M.S., Warren, R.A. & Jakob, C. (2019) A steady-state model for the relationship between humidity, instability, and precipitation in the tropics. *Journal of Advances in Modeling Earth Systems*, 11, 3973–3994.
- Sobel, A.H., Nilsson, J. & Polvani, L.M. (2001) The weak temperature gradient approximation and balanced tropical moisture waves. *Journal of the Atmospheric Sciences*, 58, 3650–3665.

- Tiedtke, M. (1989) A comprehensive mass flux scheme for cumulus parameterization in large-scale models. *Monthly Weather Review*, 117, 1779–1800.
- Tulich, S.N. & Mapes, B.E. (2010) Transient environmental sensitivities of explicitly simulated tropical convection. *Journal of the Atmospheric Sciences*, 67, 923–940.
- Wang, Z. (2020) A method for a direct measure of entrainment and detrainment. *Monthly Weather Review*, 148, 3329–3340.
- Williams, A.I.L., Jeevanjee, N. & Bloch-Johnson, J. (2023) Circus tents, convective thresholds, and the non-linear climate response to tropical SSTs. *Geophysical Research Letters*, 50, e2022GL101499.
- Williams, E. & Renno, N. (1993) An analysis of the conditional instability of the tropical atmosphere. *Monthly Weather Review*, 121, 21–36.
- Wu, G., He, B., Liu, Y., Bao, Q. & Ren, R. (2015) Location and variation of the summertime upper-troposphere temperature maximum over South Asia. *Climate Dynamics*, 45, 2757–2774.
- Xu, K.-M. & Emanuel, K.A. (1989) Is the tropical atmosphere conditionally unstable? *Monthly Weather Review*, 117, 1471–1479.
- Yang, D., Zhou, W. & Seidel, S.D. (2022) Substantial influence of vapour buoyancy on tropospheric air temperature and subtropical cloud. *Nature Geoscience*, 15, 781–788.

How to cite this article: Palmer, L.A. & Singh, M.S. (2024) The horizontal and vertical controls on the thermal structure of the tropical troposphere. *Quarterly Journal of the Royal Meteorological Society*, 150(765), 5548–5560. Available from: <https://doi.org/10.1002/qj.4888>